Physical Studies of Homologous *trans*-4-Ethoxy-4′-*n*-alkanoyloxyazobenzenes. Calorimetry

Craig L. Hillemann,[1a] Gerald R. Van Hecke,* and (in part) S. Robert Peak, John B. Winther,[1b] Martin A. Rudat,[1b] David A. Kalman,[1b] and Martha L. White

Department of Chemistry, Harvey Mudd College, Claremont, California 91711 *(Received November 15, 1974; Revised Manuscript Received April 2, 1975)*

Publication costs assisted by Harvey Mudd College

Calorimetric data are presented for the homologous *trans*-4-ethoxy-4′-*n*-alkanoyloxyazobenzenes. The extensive solid state polymorphism exhibited by this series is discussed in terms of free energy–temperature diagrams. Trends in the nematic–isotropic temperature and entropy data are discussed within the framework of current theories.

1. Introduction

As pointed out recently by van der Veen et al. very few calorimetric studies of homologous mesomorphic compounds have been reported.[2a] With the view of providing such calorimetric data, some time ago we began to study the homologous nematogens *trans*-4-ethoxy-4′-*n*-alkanoyloxyazobenzenes (I) first reported by Vorländer.[2b] Subsequent to our beginning these studies Neff et al. reported a polymorphism in the solid state of the heptanoate homolog.[3,4] Solid state polymorphism occurs frequently in this homologous series as will be discussed. McCaffrey and Castellano reported the synthesis and transition temperatures for the acetate to octanoate homologs but no calorimetric data.[5] This paper will be the first in a series reporting the results of various physical measurements for this homologous series from pentanoate to tetradecanoate. Here we present the calorimetric data and discuss the results in light of some current theories of the nematic mesophase.

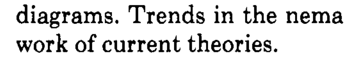

I

2. Experimental Section

Preparation of trans-4-Ethoxy-4′-n-alkanoyloxyazobenzenes. The pentanoate, hexanoate, and heptanoate esters obtained from Eastman Organic Chemicals were used after three recrystallizations from ethanol. The other esters were prepared from *p*-(*p*′-ethoxyphenylazo)phenol and the respective acyl chlorides. The compounds proved to be the trans isomer when checked by the uv spectrum technique of Neff et al. The acyl chlorides were prepared by refluxing the respective carboxylic acids with thionyl chloride and subsequent vacuum distillation. In a typical ester synthesis 8.26 mmol of the acyl chloride was added slowly by syringe to 2.00 g (8.26 mmol) of the *p*-(*p*′-ethoxyphenylazo)phenol dissolved in 15 ml of ice-cold pyridine in a flask flushed with nitrogen. After several hours the mixture was added to 100 ml of ice-cold, 1 *M* H_2SO_4, collected, washed with 200 ml of cold water, and subsequently recrystallized three times from ethanol. Final yields were about 45% with about 90% recovery per recrystallization.

Preparation of p-(p′-Ethoxyphenylazo)phenol. Eastman *p*-phenetidine (50.0 g, 0.365 mol, used without further purification) was added to 150 ml of 6 *F* hydrochloric acid, the resulting mixture cooled to 0° by the addition of ice, and a sodium nitrite solution (27.5 g in 750 ml of water, 0.398 mol) was added in small portions. After each addition the solution was checked with potassium iodide–starch paper to indicate the end point. The resulting diazonium chloride was added slowly to an ice bath-cooled phenolate solution prepared by the addition of 34.5 (0.365 mol) of phenol to 38.5 g (0.365 mol) of sodium carbonate in 350 ml of water. The golden-yellow product was acidified to pH 7 and extracted into chloroform. After drying with magnesium sulfate and removal of ether, the product was recrystallized from benzene. Recrystallized yield was 41.2 g (0.17 mol or 46.6%).

Anal.[6] Pentanoate (calcd for $C_xH_yN_2O_3$: C, 69.90; H, 6.81. Found C, 70.07; H, 7.71). Hexanoate (calcd: C, 70.53; H, 7.12. Found C, 71.02; H, 7.45). Heptanoate (calcd: C, 71.15; H, 7.41. Found C, 71.66; H, 7.85). Octanoate (calcd: C, 71.70; H, 7.67. Found C, 72.21; H, 7.55). Nonanoate (calcd: C, 72.21; H, 7.92. Found C, 72.03; H, 7.93). Decanoate (calcd: C, 72.68; H, 8.15. Found C, 72.03; H, 8.12). Undecanoate (calcd: C, 73.12; H, 8.36. Found C, 72.15; H, 8.40). Dodecanoate (calcd: C, 73.54; H, 8.56. Found C, 73.16; H, 8.88). Tridecanoate (calcd: C, 73.92; H, 8.75. Found C, 73.48; H, 8.78). Tetradecanoate (calcd: C, 74.28; H, 8.92. Found C, 74.33; H, 9.10).

Microscopy. The mesophases were identified and transition temperatures measured by the use of a Bausch and Lomb Dynoptic polarizing microscope equipped with a Nikon photographic attachment and a modified Koeffler hot stage.[7] The temperature calibration was accomplished by use of Aldrich zone-refined (99.9% +) melting point standards. The thermometric accuracy was estimated to be at least ±0.1°.

Calorimetric Measurements. The phase transition enthalpies and temperatures were determined using a Perkin-Elmer DSC-1B differential scanning calorimeter. The temperature was calibrated using the same standards as above. The instrument constant was determined using Alfa Inorganics m5n indium powder assuming a heat of fusion of 6.80 cal/g.[8] The heats of transition were obtained by photocopying, cutting, and weighing, or planimetry of the peak areas. The following technique was used to determine the peak shape for area measurement. The initial and final

TABLE I: Transition Temperatures, Enthalpies, and Derived Entropies for 4-Ethoxy-4′-*n*-alkanoyloxyazobenzenes

Ester	Transition[a]	Temp ref[b]	Temp, K: M[c]	Temp, K: V[c]	Temp, K: Present	$\Delta\bar{H}$, kJ mol^{-1}	$\Delta\bar{S}$, J mol^{-1} K^{-1}
Pentanoate	$K_{III} \rightarrow N$	T4	351	352	352.02 ± 0.09	33.2 ± 1.1	94 ± 3
	$N \rightarrow I$	T7	399	398	400.2 ± 0.1	0.88 ± 0.03	2.19 ± 0.07
Hexanoate	$K_{III} \rightarrow N^{e}$	T4	341	343	339.11 ± 0.05	37.3 ± 0.8	108 ± 3
	$K_{I} \rightarrow N^{f}$	T6			345.08 ± 0.25	29.8 ± 0.7	88 ± 2
	$N \rightarrow I$	T7	400	399	401.6 ± 0.1	1.13 ± 0.06	2.82 ± 0.15
Heptanoate	$K_{III} \rightarrow N$	T4	337	341	333.74 ± 0.17	*d*	*d*
	$K_{I} \rightarrow N$	T6			338.74 ± 0.11	23.1 ± 1.8	68 ± 5
	$N \rightarrow I$	T7	390	391	392.3 ± 0.1	0.91 ± 0.02	2.33 ± 0.06
Octanoate	$K_{III} \rightarrow N$	T4	360	360	358.95 ± 0.21	48.1 ± 1.4	134 ± 4
	$N \rightarrow I$	T7	391	391	392.8 ± 0.1	1.11 ± 0.03	2.82 ± 0.08
Nonanoate	$K_{III} \rightarrow K_{II}{}^{g}$	T1			333.92 ± 0.38	13.7 ± 0.3	38 ± 1
	$K_{II} \rightarrow K_{I}$	T3			342.7 ± 1.0	*d*	*d*
	$K_{II} \rightarrow N$	T5			343.26 ± 0.10	28.8 ± 1.8	84 ± 5
	$K_{I} \rightarrow N^{h}$	T6		345	345.46 ± 0.20	27.7 ± 1.6	80 ± 5
	$N \rightarrow I$	T7		385	387.7 ± 0.1	0.93 ± 0.03	2.39 ± 0.06
Decanoate	$K_{III} \rightarrow K_{II}{}^{i}$	T1			~337	*d*	*d*
	$K_{II} \rightarrow K_{I}{}^{i}$	T3			~343	*d*	*d*
	$K_{III} \rightarrow N$	T4			344.56 ± 0.10	45.8 ± 1.3	133 ± 4
	$K_{II} \rightarrow N^{j}$	T5			346.92 ± 0.06	32.1 ± 0.7	93 ± 2
	$K_{I} \rightarrow N^{i}$	T6		348	348.6 ± 0.2	*d*	*d*
	$N \rightarrow I$	T7		386	386.1 ± 0.1	1.10 ± 0.03	2.85 ± 0.09
Undecanoate	$K_{II} \rightarrow K_{I}{}^{i}$	T3			~348	*d*	*d*
	$K_{II} \rightarrow N$	T5			350.44 ± 0.10	31.9 ± 0.9[k]	91 ± 3
	$K_{I} \rightarrow N^{i}$	T6		351	352.2 ± 0.2		
	$N \rightarrow I$	T7		382	383.1 ± 0.1	0.98 ± 0.05	2.56 ± 0.12
Dodecanoate	$K_{II} \rightarrow N$	T5			352.35 ± 0.12	38.9 ± 0.6[k]	110 ± 2
	$K_{I} \rightarrow N^{i}$	T6		354	353.8 ± 0.3		
	$N \rightarrow I$	T7		381	382.5 ± 0.1	1.17 ± 0.04	3.05 ± 0.07
Tridecanoate	$K_{II} \rightarrow N$	T5		351	355.80 ± 0.07	41.7 ± 0.8[k]	117 ± 2
	$K_{I} \rightarrow N^{i}$	T6			356.5 ± 0.3		
	$N \rightarrow I$	T7		378	379.7 ± 0.1	1.16 ± 0.04	305 ± 0.09
Tetradecanoate	$K_{II} \rightarrow N$	T5			357.80 ± 0.09	43.2 ± 0.9[k]	121 ± 2
	$K_{I} \rightarrow N^{i}$	T6		356	358.3 ± 0.3		
	$N \rightarrow I$	T7		376	379.4 ± 0.1	1.31 ± 0.04	3.43 ± 0.10

[a] Notation of Verbit ref 10: K = crystal, N = nematic, I = isotropic. [b] Temp ref code refers to the transitions depicted in Figure 1. T6 means temperature of point 6, the $K_I \rightarrow N$ transition Figure 1. [c] M is data of McCaffrey and Castellano, ref 5; V is data of Vorländer, ref 2b. [d] Value not reported for lack of suitable resolution or reproducibility of DSC curves. [e] DSC: previously melted and cooled to 320 K for 15 min. [f] DSC: previously allowed to stand at room temperature for more than 9 hr. [g] DSC: previously allowed to stand at 312 K for 2 hr. [h] DSC: previously allowed to stand at 336 K for 15 min. [i] Temperatures determined by microscope; by DSC event could not be observed or not resolved. [j] DSC: the ester was previously allowed to stand at 343 K for 30 min. Under these conditions no formation of K_I was detectable. [k] Values reported are for two transitions.

baselines were respectively extrapolated to the initial transition temperature and to the final transition temperature. The effect of the heat capacity variation occurring between these temperatures was estimated by then drawing a line joining the intersections just defined above. The precision estimates were calculated on the basis of repetitive runs and samples.

Several esters, as will be discussed, possess crystal modifications which are thermodynamically unstable relative to other crystal forms near their melting points. The rate of crystal–crystal transformation, though usually slow in the solid phase, is rapid in the presence of the liquid nematic, often resulting in an endotherm–exotherm–endotherm DSC thermogram. The enthalpy of fusion of the less stable crystal is calculated by summing the areas of the endotherm peaks and subtracting the area corresponding to the exotherm. The more stable crystal can be exclusively obtained by heating the ester at such a temperature as to melt the less stable but not the more stable crystal modification. Its enthalpy of fusion can then be easily determined from a single endothermic DSC peak.

3. Results

The combined results of the microscopic and calorimetric studies are presented and correlated with previous data in Table I. Each homolog exhibits only an enantiotropic nematic mesophase. However, considerable polymorphism is exhibited in the solid state by most of the homologs, and before further discussion of general trends, the peculiarities of each homolog will be delineated.

4-Ethoxy-4′-n-pentanoyloxyazobenzene (*Pentanoate*). Our transition temperatures agree to within implied experimental uncertainty of literature values. The pentanoate is one of two homologs that do not show solid state polymorphism. Figure 1 presents an idealized free energy diagram capable of describing the many phases observed for these

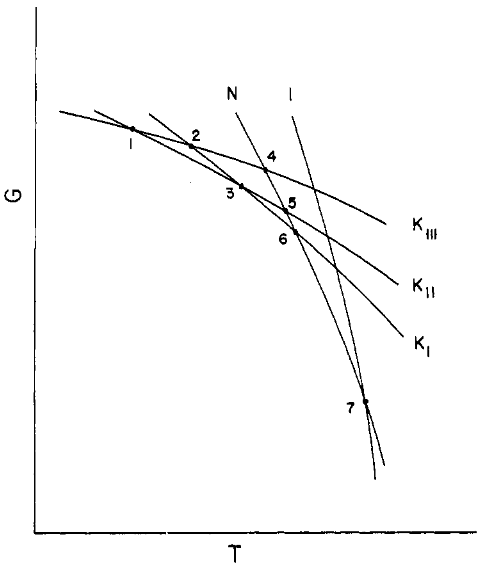

Figure 1. Idealized free energy–temperature diagram. Slopes and temperature differences are exaggerated for clarity. The notation of Verbit (ref 10) is used.

compounds.[9] Neff et al. used a diagram similar to Figure 1 to explain the anomalous melting of the heptanoate ester. Here for pentanoate the observed phase transitions would be described by lines K_{III}, N, and I and their temperature intersection points T4 and T7.[10] Calling the crystal K_{III} is not arbitrary since there is a trend in the types of crystalline phases observed in the series as will be discussed later.

4-Ethoxy-4′-n-hexanoyloxyazobenzene (*Hexanoate*). The nematic–isotropic transition temperature reasonably well agrees with literature values, our value being slightly higher. Hexanoate shows two crystal forms and in Figure 1 the appropriate free energy lines are K_{III}, K_I, N, and I. With reference to Table I, no well-defined temperature for the $K_{III} \rightarrow K_I$ transition can be reported since the K_I crystal form is thermodynamically stable relative to K_{III} from its melting point to below room temperature, at which point the rate of conversion is even too slow to be studied microscopically. The literature values for the crystal–nematic temperature appear to be for $K_I \rightarrow N$. Striking evidence for the existence of two crystals is provided by DSC. When the K_{III} crystal is initially present the DSC curves usually appear as in Figure 4. At slow heating rates (less than 2.5°/min) this endothermic–exothermic behavior is often observed since at such rates the nematic phase obtained from $K_{III} \rightarrow N$ can be superheated past T4 (Figure 1) with accompanying $N \rightarrow K_I$ and then $K_I \rightarrow N$ at T6. Not infrequently, however, $K_{III} \rightarrow N$ is solely observed. Since the exothermic–endothermic phenomenon is never observed for heating rates greater than 2.5°/min, McCaffrey and Castellano could not have been expected to see the conversions at their 10°/min heating rate even if K_{III} were present.

4-Ethoxy-4′-n-heptanoyloxyazobenzene (*Heptanoate*). The nematic–isotropic transition temperatures agree well with the literature. Heptanoate exhibits two crystal forms of the same appearance as hexanoate. For the heptanoate ester K_{III} is evidently the thermodynamically stable form at room temperature. The behavior of this compound was first discussed by Neff et al. The observation of the endothermic–exothermic DSC curve (of the type depicted in Figure 4) is also dependent on heating rate.

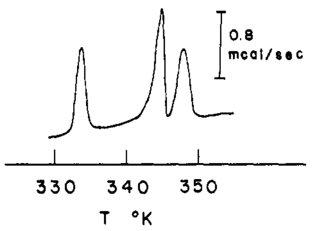

Figure 2. A first heating DSC curve obtained at 2.5°/min for 4-ethoxy-4′-*n*-nonanoyloxyazobenzene.

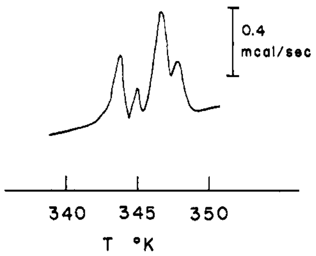

Figure 3. A heating DSC curve obtained at 1.25°/min for 4-ethoxy-4′-*n*-nonanoyloxyazobenzene.

4-Ethoxy-4′-n-octanoyloxyazobenzene (*Octanoate*). Octanoate is the other member of this series that exhibits only one crystal form. The transition temperatures agree well with the literature, though again our nematic–isotropic temperature is slightly higher. The free energy diagram is the same as that for pentanoate: K_{III}, N, and I.

4-Ethoxy-4′-n-nonanoyloxyazobenzene (*Nonanoate*). The nematic–isotropic transition temperature is not in good agreement with Vorländer, his value being almost 3° lower, perhaps indicating purity differences. On the other hand, nonanoate exhibits the most complex solid state polymorphism observed in this series. Three crystal modifications have been observed microscopically and resolved by DSC experiments. The free energy diagram is given by all lines in Figure 1. The usefulness, if not the necessity, of such a diagram to assist the understanding of these systems is demonstrated in sorting out the observed DSC behavior, examples of which are given in Figures 2 and 3. Figure 2 is a first heating curve obtained at 2.5°/min. The endothermic events observed are, in order of increasing temperature, $K_{III} \rightarrow K_{II}$, $K_{II} \rightarrow K_I$, and $K_I \rightarrow N$. Agreement of the transition temperatures determined microscopically and by DSC is excellent. Different curves can result since the extent of the interconversion of crystal forms is dependent on sample treatment. Here also the kinetics of interconversion are rapid enough to watch microscopically. The explanation of the DSC curve in Figure 3 obtained at 1.25°/min is, in order of increasing temperature, $K_{II} \rightarrow K_I$, unconverted $K_{III} \rightarrow N$, unconverted $K_{II} \rightarrow N$, and finally $K_I \rightarrow N$. Thus in this experiment the system, which can exist in several metastable states at the same time because of kinetic factors, started initially as a mixture of K_{III} and K_{II} which simply followed possible free energy paths through transitions marked T3, T4, T5, and T6 in Figure 1. Ready explanation of the variety of DSC curves obtained and microscopic transitions observed would be difficult at best without Figure 1. The reported crystal–nematic transition of Vorländer appears to be that for $K_I \rightarrow N$ which is plausible for only visual observation.

4-Ethoxy-4′-n-decanoyloxyazobenzene (*Decanoate*).

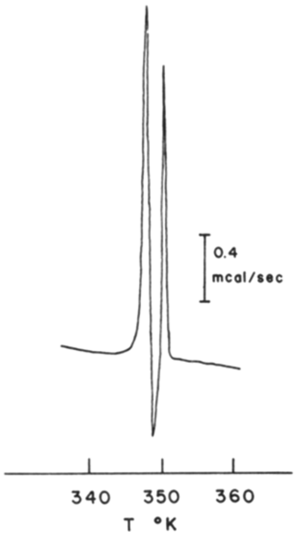

Figure 4. A heating DSC curve obtained at 2.5°/min for 4-ethoxy-4′-*n*-decanoyloxyazobenzene.

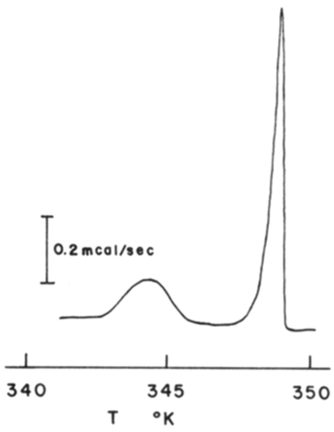

Figure 5. A heating DSC curve obtained at 0.625°/min for 4-ethoxy-4′-*n*-decanoyloxyazobenzene.

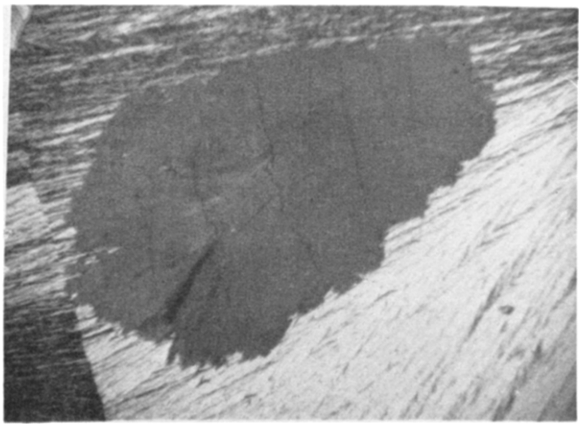

Figure 6. A photomicrograph, 50X at film plane, of the K_{II} (sheet) and K_I (spherlite) crystalline modifications of 4-ethoxy-4′-*n*-dodecanoyloxyazobenzene.

The nematic–isotropic transition temperature is in excellent agreement with literature. Decanoate also exhibits three crystalline modifications which can be clearly discerned microscopically. However, the kinetics of transformation between these phases make the dynamic experiment, DSC, more difficult to sort out in contrast to nonanoate results. Figure 4 shows a DSC curve reminiscent of those observed for hexanoate and heptanoate. Here the explanation is analogous to that for the previous cases. However, if the heating rate is slowed down quite different DSC curves are obtained for decanoate compared to the lower homologs as might well be expected. Figure 5 shows the result of one run at 0.625°/min. Now with increasing temperature $K_{II} \rightarrow K_I$ and then $K_I \rightarrow N$. Again the free energy diagram is extremely useful in interpreting experimental results. The reported crystal–nematic temperature of Vorländer here also appears to be for $K_I \rightarrow N$.

4-Ethoxy-4′-n-undecanoyloxyazobenzene (*Undecanoate*). The nematic isotropic transition temperature agrees to within implied error with literature. Undecanoate exhibits two crystal modifications K_{II} and K_I. For the higher homologs the lower temperature crystal is K_{II} while for the lower homologs K_{III} is the stable low temperature crystal. Experimentally the crystal–crystal transition was undetectable by DSC and the $K_{II} \rightarrow N$ and $K_I \rightarrow N$ transitions are too close to be resolved. The $K_{II} \rightarrow K_I$ transition (both heating and cooling) is observable visually but no distinct temperature could be assigned. The free energy diagram is given by lines K_{II}, K_I, N, and I, and the calorimetric results reported in Table I for the $K_{II} \rightarrow N$ transition undoubtedly contains to some degree the $K_I \rightarrow N$ transition as well.

4-Ethoxy-4′-n-dodecanoyloxyazobenzene (*Dodecanoate*). The nematic–isotropic transition temperature agrees with the literature value. Dodecanoate exhibits the same solid state polymorphism as undecanoate with the same lack of resolution of the $K_{II} \rightarrow N$, $K_I \rightarrow N$ transitions and the unobserved (DSC) $K_{II} \rightarrow K_I$ transition. The shoulders often observed on the DSC $K_{II} \rightarrow N$ peak strongly suggest the unresolved nature of this transition. The inability to resolve these transitions compared to the hexanoate and the heptanoate cases is explained by the only 0.5° difference in the transitions for dodecanoate vs. the 5–6° difference for the previous compounds. Figure 6 is a photomicrograph of the two crystal forms coexisting at 22°. The smooth, sheet-like crystal we have been calling K_{II}, while the spherlite crystal surrounding it has been called K_I.

4-Ethoxy-4′-n-tridecanoyloxyazobenzene (*Tridecanoate*). The results and discussion are analogous to that of undecanoate and dodecanoate.

4-Ethoxy-4′-n-tetradecanoyloxyazobenzene (*Tetradecanoate*). The results are the same as those discussed for undecanoate and dodecanoate.

4. Discussion

Crystal–Nematic Transitions. The curious feature of this homologous series of azobenzenes is the extensive solid state polymorphism. There are trends in the types of crystals observed which are detailed in Table II. Since the morphology of the crystals is not known, the various modifications are simply described by names appropriate to their microscopic appearance. These crystal modifications have been previously called K_{III}, K_{II}, and K_I for star, sheet, and spherlite, respectively. The regular change is obvious but unexplained. The octanoate homolog stands out, however, exhibiting only one crystal form, though the nearest homologs, heptanoate and nonanoate, exhibit complex polymorphism. In Figures 7 and 8 are plotted the transition tem-

TABLE II: Trends in the Observed Solid State Polymorphism of 4-Ethoxy-4′-*n*-alkanoyloxyazobenzenes

	Star (K_{III})	Sheet (K_{II})	Sphelite (K_I)
Pentanoate	X		
Hexanoate	X		X
Heptanoate	X		X
Octanoate	X		
Nonanoate	X	X	X
Decanoate	X	X	X
Undecanoate		X	X
Dodecanoate		X	X
Tridecanoate		X	X
Tetradecanoate		X	X

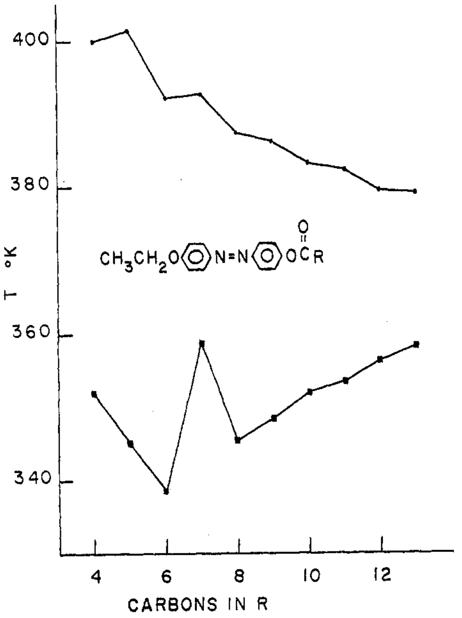

Figure 7. Transition temperatures K_I to N and N to I as a function of carbon number in alkyl chain of 4-ethoxy-4′-*n*-alkanoyloxyazobenzenes.

peratures and calorimetric data and here again the octanoate appears to be out of place. The $K_I \to N$ transition temperature especially appears anomalously high. Other homologous series based on the normal alkanes also show this anomaly. For example, the amides of the *n*-alkyl carboxylic acids show the greatest variation in melting point around the eight carbon chain.[11] Apparently for the eight carbon homolog in many derivatives of these aliphatic acids the crystal packing must give rise to larger intermolecular crystalline forces

Few theoretical studies have been made of the crystal–nematic transition. Chandrasekhar et al. have done a statistical calculation which does predict at least two possible solid state transitions for various values of a parameter measuring the relative barriers to rotation and diffusion in the crystal.[12] Either, a solid–solid rotational transition precedes the melting (to nematic) transition, or some type of positional transition occurs prior to melting. For most of the homologs here two transitions are observed, but it is not known whether the nature of the transition is rotational or positional. Morcover the theory, at least within the model of one parameter, cannot account for the three observed transitions for the nonanoate and decanoate homologs. For the one case where the ΔS for a solid–solid transition could be measured, $K_{III} \to K_{II}$ for nonanoate, a value of 38 J/mol K was obtained which is very much larger than the values noted by Chandrasekhar et al. Also the $\Delta S/R$ values for the crystal–nematic transition are in the range of 10–12 in rough agreement with other materials but in poor agreement with theory. Hijikuro et al. give a theoretical treatment of the crystal–nematic transition that can predict a solid phase which is orientationally disordered, corresponding to a rotational transition, as well as a melting to the nematic positionally disordered state.[13] X-Ray studies might better define the nature of the transitions as Wendorff and Price have done for several esters of cholesterol.[14]

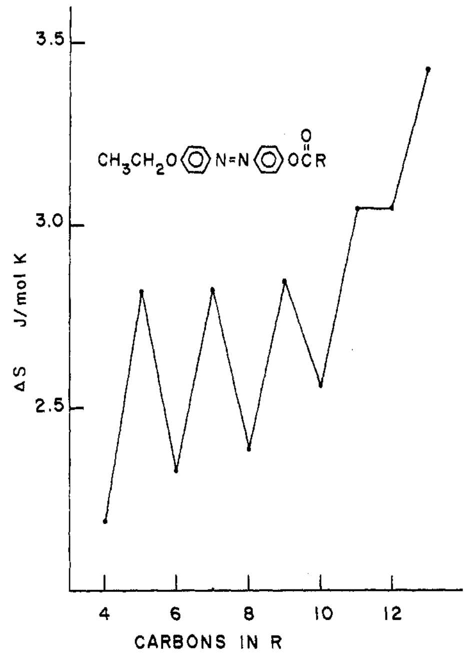

Figure 8. Entropy of N to I transition as a function of carbon number in alkyl chain of 4-ethoxy-4′-*n*-alkanoyloxyazobenzenes.

Nematic–Isotropic Transitions. Only enantiotropic nematic mesophases are observed for this series notwithstanding Vorländer's report of monotropic phases. The lack of smectic phases is surprising since, for essentially all homologous series of liquid crystalline materials reported in the literature, once the alkyl chain length becomes longer than eight carbons, smectic mesophases occur. For this series of azobenzenes McCaffrey and Castellano explain this lack of smectics by the absence of a transverse dipole. However, this suggestion seems doubtful as many new compounds, for example, several cyanobiphenyl derivatives, have no transverse dipole yet often exhibit extensive smectic mesomorphism.[15] The lack of smectic phases for the higher homologs of this series still seems unexplained.

A regular alternation of increasing nematic–isotropic transition temperature, T_{NI}, on going from even to odd is observed in Figure 7 up to C8. Past C8 T_{NI} always decreases but still in an alternate manner. Vorländer's data show a regular increase in T_{NI} going from even to odd until past C13 at which point T_{NI} decreases for even to odd. Several possible explanations for the uniform alternation exist in the literature but none attempt to account for the reversal. Kaplan describes T_{NI} as a function of the intermolecular potential which in turn is a function of molar volume $T_{NI} \propto AV^{-n}$, where V is the molar volume and A is a parameter from Maier–Saupe theory.[16,17] Since T_{NI} is observed to alternate, either A or the molar volume must alternate. It is unlikely that the molar volume is anything but a smooth function of chain length, and moreover, de Jeu et al. point out that A does alternate with chain length and reflects a change in the anisotropy of the polarizability.[18] Stenschke relates T_{NI} to a characteristic energy, Δ, reflecting the energy difference between alkyl chain trans and gauche conformations.[19] The alternation of T_{NI} then becomes an alternation of Δ on going from odd to even vs. even to odd when adding carbons to the chain. Marcelja has quantified this approach by calculating all the conformational energies accessible to a zig-zag alkane chain and noting that the alternation is indeed due to the change in anisotropic properties of the molecule engendered on the odd to even vs. the even to odd change.[20] Marcelja's work provides a rationale for the previous suggestions in that the Maier–Saupe parameter A does depend on anistropy differences in polarizability, and the trans–gauche interaction energy does change alternating down the chain. Further, the temperature drop with increasing chain length observed for this series is explained in Marcelja's calculation by the weakening of the strong forces between the central azobenzene groups caused by the increasing alkyl chains.

The odd–even variation of ΔS_{NI} with chain length depicted in Figure 8 is much more marked than the T_{NI} variation. The marked alternation here has its origin in the fact that ΔH_{NI} alternates markedly and in the same manner as T_{NI} (not surprisingly). With Young et al. we note that the increment of ΔS_{NI} with chain length is much less than R ln 3 which suggests that the nematic phase alkyl chain cannot exist in a single conformation.[21] This argument is confirmed by Marcelja's results. The prediction by van der Veen et al. that the variation of ΔS_{NI} with chain length reflects the variation in the order parameter is also suggested by Marcelja's calculations but no experimental order parameter data exists to check this. The variation in the order parameter might also simply be a reflection of the variation of the Maier–Saupe A. Work is in progress to test the variation of order parameter with chain length.

Acknowledgments. The authors thank Edward Newton for assistance in the design of the microscope hot stage. Financial support from the National Science Foundation through its Undergraduate Research Participation Program, the Harvey Mudd College Research Committee, and the Cal Biochem Research Foundation is gratefully acknowledged.

References and Notes

(1) (a) Cal Biochem undergraduate research fellow. (b) NSF undergraduate research participant.
(2) (a) J. van der Veen, W. H. de Jeu, M. W. M. Wanninkhof, and C. A. M. Teinhoven, *J. Phys. Chem.*, **77**, 2153 (1973), and references therein; (b) D. Vorländer, *Z. Phys. Chem.* (*Liepzig*), **126**, 449 (1927).
(3) V. D. Neff, M. K. Chang, and D. L. Fishel, *Mol. Cryst. Liq. Cryst.*, **17**, 369 (1972).
(4) We will call the individual homologs by their systematic parent acids name. Hence the seven carbon containing C–R homolog will be called heptanoate.
(5) M. T. McCaffrey and J. A. Castellano, *Mol. Cryst. Liq. Cryst.*, **18**, 209 (1972).
(6) Chemalytics, Inc., Tempe, Ariz. 85281.
(7) The Koeffler hot stage was modified with a constant temperature controller capable of holding the temperature to better than ±0.05° and built for less than $40. Details on request.
(8) G. J. Davis, R. S. Porter, and E. M. Barrall, II, *Mol. Cryst. Liq. Cryst.*, **10**, 1 (1970).
(9) W. C. McCrone in "Physics and Chemistry of the Organic Solid State", D. Fox, M. M. Labes, and A. Weissberger, Ed., Interscience, New York, N.Y., 1965, Chapter 8.
(10) L. Verbit, *Mol. Cryst. Liq. Cryst.*, **15**, 89 (1971).
(11) Data selected from "Handbook of Tables for Organic Compound Identification", 3rd ed, Chemical Rubber Publishing Co., Cleveland, Ohio, 1967.
(12) S. Chandrasekhar, R. Shashidhar, and N. Tara, *Mol. Cryst. Liq. Cryst.*, **10**, 337 (1970); **12**, 245 (1971).
(13) N. Hijikuro, K. Miyakawa, and H. Mori, *Phys. Lett.*, **45A**, 257 (1973), and references therein.
(14) J. H. Wendorff and F. P. Price, *Mol. Cryst. Liq. Cryst.*, **25**, 71 (1974).
(15) G. W. Gray, paper given at the Vth International Liquid Crystal Conference, Stockholm, Sweden, 1974.
(16) J. I. Kaplan, *J. Chem. Phys.*, **57**, 3015 (1972).
(17) W. Maier and A. Saupe, *Z. Naturforsch A*, **14**, 882 (1959); **15**, 287 (1960).
(18) W. H. de Jeu, J. van der Veen, and W. J. A. Goossens, *Solid State Commun.*, **12**, 405 (1973).
(19) H. Stenschke, *Solid State Commun.*, **10**, 653 (1972).
(20) S. Marcelja, *J. Chem. Phys.*, **60**, 3599 (1974).
(21) W. R. Young, I. Haller, and A. Aviram, *IBM J. Res. Develop.*, **15**, 41 (1971).